Electronic Supplementary Material (ESI) for Physical Chemistry Chemical Physics
This journal is © The Owner Societies 2013

Electronic Supplementary Information

Aqueous Semi-Solid Flow Cell: Demonstration and Analysis

Zheng Li,[a‡] Kyle C. Smith,[a‡] Yajie Dong,[a] Nir Baram,[a] Frank Fan,[a] Jing Xie,[a] Pimpa Limthongkul,[c] W. Craig Carter[a] and Yet-Ming Chiang[a]*

**Corresponding author's e-mail: ychiang@mit.edu*
[a] Department of Materials Science and Engineering, Massachusetts Institute of Technology, Cambridge, MA 02139, USA.
[c] 24M Technologies, Inc., One Kendall Square Suite B6103, Cambridge MA 02139, USA.
‡ Zheng Li and Kyle C. Smith contributed equally to this work.

Experimental Details

Materials. The cathode materials LFP (Advanced Lithium Electrochemistry Co., Ltd., Taiwan) and LMO (Toda, Japan) were used as received. LTP and LTP-C were synthesized by solid-state reactions. Stoichiometric amount of Li_2CO_3 (Alfa Aesar, USA), TiO_2 (Sigma Aldrich, USA) and $NH_4H_2PO_4$ (Alfa Aesar, USA) were mixed by Spex Mixer/Mill® using zirconia ceramic milling media in ethanol for 1 h, followed by drying and calcining at 500 °C for 6 h in air. A final heat treatment was done at 900 °C for 12 h in air. For LTP-C, the as-synthesized LTP was roller ball-milled with glucose in a mass ratio of 9:1 in distilled water for 14-15 days. The dried mixture was pelletized and fired at 800 °C for 3 h in flowing Ar, targeting 2-3% pyrolytic carbon in the final composite.

Materials characterization. The XRD patterns of LTP and LTP-C were obtained using a PANalytical X'Pert Pro multipurpose diffractometer equipped with a Cu-K_α radiation and X'Celerator detector. The morphology of LTP and LTP-C were examined using JEOL 5910 General Purpose SEM and FEI/Philips XL30 Field Emission Gun Environmental SEM.

Semi-solid suspension preparation. The active materials and Ketjen Black (Azko Nobel Polymer Chemicals LLC, USA) were homogenously mixed in glass vials before adding the aqueous electrolyte, 1M $LiNO_3$ (Sigma Aldrich, USA), pH = 11~12. The pH was adjusted by adding LiOH (Alfa Aesar, USA). The suspension was sonicated for 15 min before use.

Cell construction and electrochemical measurement. Modified Swagelok cells were used for static suspension tests. Wells with 0.25 mm depth were drilled into current collector metal parts (Ni for cathode and Stainless Steel for anode) to hold the suspension. The Swagelok cells were either assembled in an Ar-filled glovebox or in air. For the intermittent flow test, the flow cell reactor was made of PVDF with nickel and stainless steel wires attached to the external circuit. The geometry of the flow channel designs are shown in previous publications from this group.[1,2] The electroactive region of the flow channel exhibits a cross-sectional area of 2.0 mm^2. The reactor was connected to syringes which serve as reservoirs to store suspension. The pushing and pulling of the syringe plungers were controlled by a neMESYS pump. For both Swagelok and flow cells, the current collectors were gold sputtered to minimize corrosion and contact resistance with the aqueous suspension. All the cells employed Celgard® 3501 as the separator and the electrochemical tests were performed on a Biologic VMP potentiostat.

Rheology and conductivity measurement. The viscosity measurement was done on a rheometer (AR2000, TA instruments, USA) with parallel plate geometry. Electronic conductivity measurements on the suspensions were performed in a two-probe parallel plate geometry. A cylindrical well in a PTFE housing was sealed on either end by polished stainless steel plates. A Solartron Analytical model 1470 potentiostat was used to apply a +/-50 mV DC bias to the parallel plates and the resistance was calculated using the measured current at steady state. The conductivity was obtained by dividing the cell factor by the resistance. The cell factors were calibrated to 1.2 cm^{-1} with a 15 mS/cm conductivity standard produced by Oakton Instruments.

Simulation Details

A two-dimensional electrochemical transport model was employed to simulate the transient behavior of intermittent flow cycles incorporating electronic conduction, intercalation kinetics, and bulk fluid motion. The rectangular domain considered is defined by an inlet region, electroactive region, and outlet region (see Fig. S5). In all cases an electroactive region of length L_{cc}=47.2mm and width w=0.40mm was considered. Inlet and outlet lengths, L_i and L_o respectively, were 141.2mm in the case of unity flow volume factor, while lengths of 282.0mm were employed for the larger flow volume factor. An anisotropic, rectilinear mesh was employed with spacing between mesh points of 0.01mm and 0.40mm in the x and y directions, respectively.

Electronic Supplementary Material (ESI) for Physical Chemistry Chemical Physics
This journal is © The Owner Societies 2013

Electronic Supplementary Information

The intermittent operation of the flow cell enables the isolation of electrochemical cycles into two distinct states governed by either (1) static electrochemical processes or (2) non-reacting suspension advection. The set of governing equations for static electrochemical processes includes electronic charge conservation in the suspension:

$$\nabla\cdot\left(-\sigma\nabla\phi_s\right)+S=0,$$

where σ is the effective electronic conductivity of the suspension for which a value of 2 mS/cm was employed in the present work. Additionally, the electrochemically active storage material embedded in the suspension is governed by the following conservation equation:

$$\frac{\partial n}{\partial t}=S.$$

Here the electronic suspension voltage, stored electronic charge density, and time are ϕ_s, n, and t, respectively. Overpotential η at the solid-electrolyte interface drives Li intercalation and is defined as ϕ_s-ϕ_e-U, where ϕ_e and U are the ionic electrolyte voltage and open-circuit potential, respectively. Butler-Volmer interface kinetics with equal anodic and cathodic transfer coefficients[3] couples electronic diffusion to electrochemical storage through the source term S:

$$S=i_0 a_s\left[\exp\left(\frac{0.5F\eta}{RT}\right)-\exp\left(-\frac{0.5F\eta}{RT}\right)\right],$$

where i_0, a_s, T, F, and R are the exchange current density, surface area per unit suspension volume, temperature, Faraday's constant, and universal gas constant, respectively. The values of exchange current density, suspension specific surface area, and temperature were $5.4\text{x}10^{-3}$ A/m^2, $2\text{x}10^6$ m^2/m^3, and 300 K, respectively. The coupling of open-circuit potential U to the charge density n was incorporated with the experimental curve reported by Kasavujulii et al.[4] for $LiFePO_4$. A high-density anode with constant voltage at 2.5 V vs. Li^+/Li that corresponds to the plateau voltage of $LiTi_2(PO_4)_3$ was considered as the counter-electrode.[5]

Non-reacting suspension advection is governing by the conservation of stored charge in the absence of electrochemical processes:

$$\frac{\partial n}{\partial t}=-\vec{u}\cdot\nabla n,$$

where $\vec{u}$ is the suspension velocity field, as indicated in Fig. S5. The Newtonian velocity profile corresponds to that of a two-dimensional Poiseuille flow without slip at current collector surfaces (x=w and x=-w):

$$\vec{u}=1.5\overline{u}\left(1-\left(\frac{x}{w}\right)^2\right)\hat{j},$$

where $\overline{u}$ and $\hat{j}$ are the mean flow velocity and unit vector along the channel's axis, respectively. Likewise, plug flows were implemented with a uniform velocity profile, $\vec{u}=\overline{u}\hat{j}$. At the inflow boundary fluid is assumed to advect with charge density equal to that just inside the boundary.

The governing equations for state (1) were discretized with the finite volume method[6] with implicit discretization in time and central difference discretization in space. Because the transfer of charge is purely advective during intermittent pumping, streamline integration was employed to solve state (2). With this approach charge density was determined by backward-time, nearest-neighbor interpolation along streamlines.

Electronic Supplementary Information

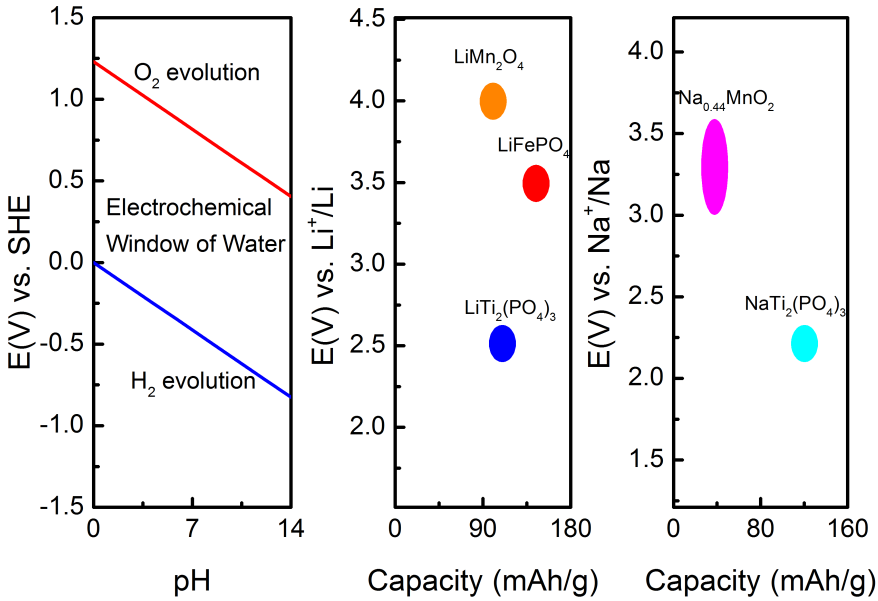

Fig. S1 Pourbaix diagram of water and Li-ion or Na-ion intercalation voltages of alkali metal-ion storage compounds that are electrode materials for aqueous rechargeable batteries. The electrochemical stability area of the aqueous electrolyte is between O_2 and H_2 evolution lines. $LiTi_2(PO_4)_3$ (LTP) and $NaTi_2(PO_4)_3$ (NTP) can be used as anode active materials, and $LiMn_2O_4$ (LMO), $LiFePO_4$ (LFP) and $Na_{0.44}MnO_2$ (NMO) as cathode active materials to prepare semi-solid suspensions. This paper uses LTP/LFP as a base case to demonstrate an aqueous semi-solid flow cell (A-SSFC).

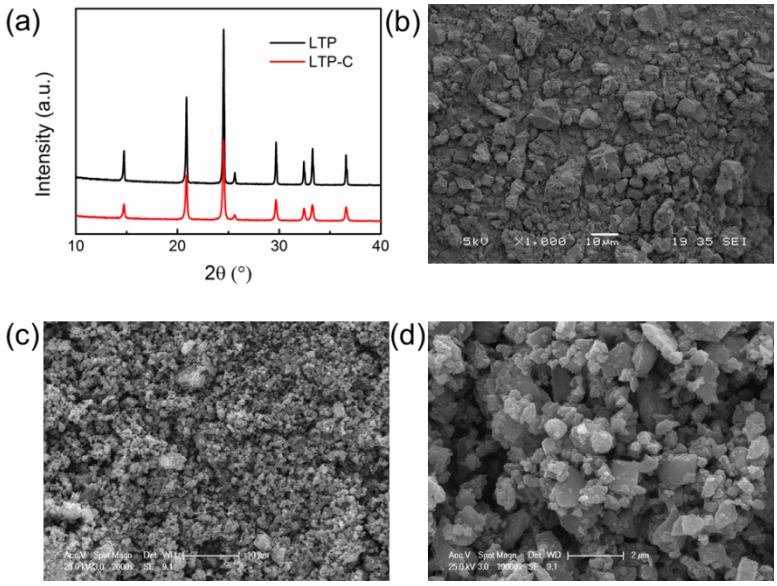

Fig. S2 (a) XRD patterns of LTP and LTP-C. (b) SEM image showing morphology of as-synthesized LTP. (c) and (d) are SEM images of LTP-C.

Electronic Supplementary Material (ESI) for Physical Chemistry Chemical Physics
This journal is © The Owner Societies 2013

Electronic Supplementary Information

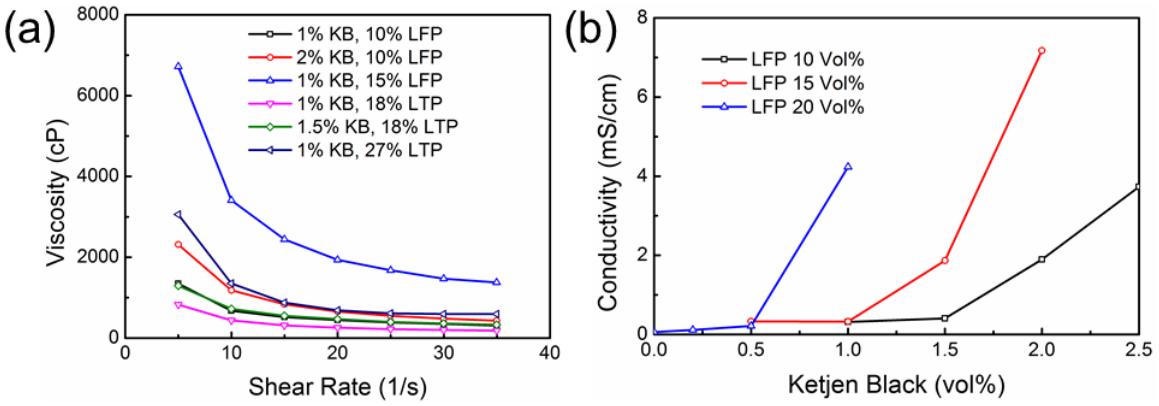

Fig. S3 (a) Viscosity versus shear rate for suspensions with 1-2 vol% KB and 10-27 vol% LFP or LTP. (b) The electronic conductivity of suspensions with 0-2.5 vol% KB and 10-20 vol% LFP.

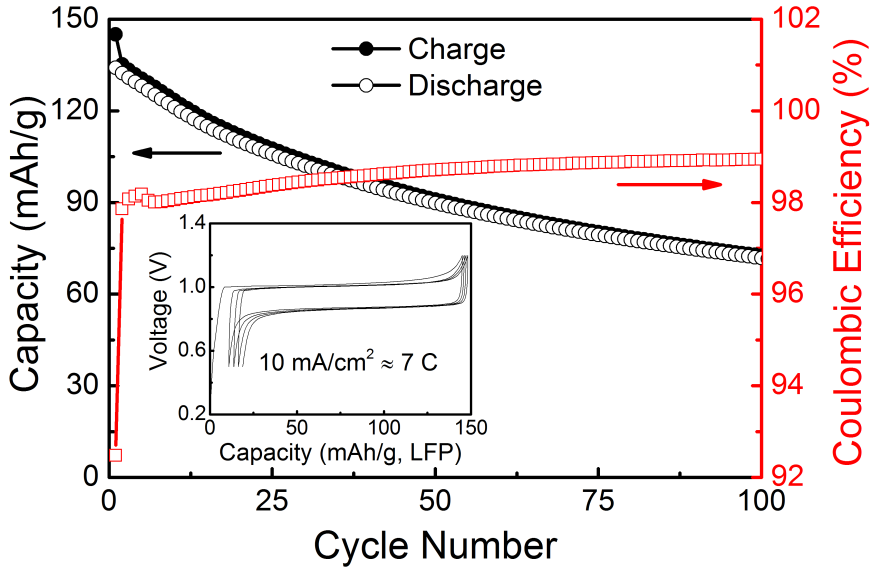

Fig. S4 The cycling performance and coulombic efficiency of the non-flowing Air-cell. The suspensions in the cell are same as those used in Fig. 1. The first charge capacity of the cell is normalized to the same value as the Ar-cell for comparison.

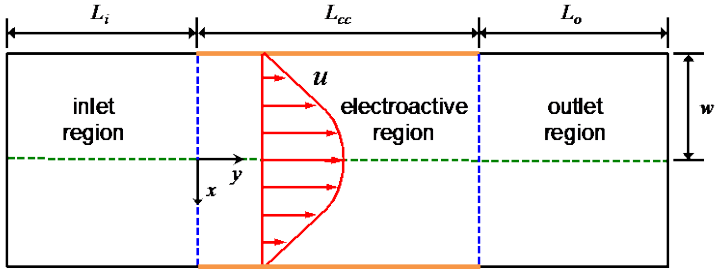

Fig. S5 Computational domain of flow cell simulations. The gold line marks the boundary at which the current collector contacts suspensions, and black lines indicate boundaries through which no diffusive fluxes pass. The electroactive region is bounded by blue-dashed lines. Dimensions of the geometry are indicated in addition to the coordinate system employed. The velocity field $\vec{u}$ induces flow in the cell.

Electronic Supplementary Material (ESI) for Physical Chemistry Chemical Physics
This journal is © The Owner Societies 2013

Electronic Supplementary Information

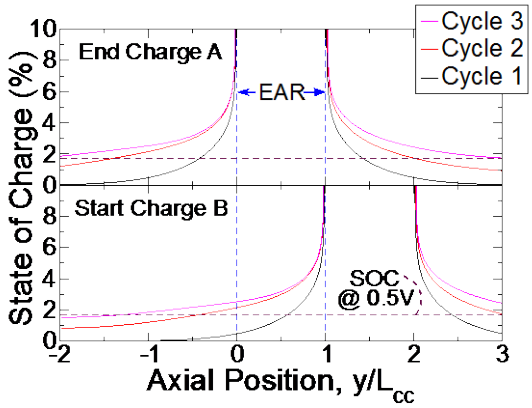

Fig. S6 Simulated state-of-charge (SOC) profiles in the LFP electrode at the end of charging aliquot A (top panel) and the start of charging aliquot B (bottom panel). The profiles shown are along the centerline of the flow channel (x=0). The curves were obtained for a rate of C/3 and unity aliquot factor with intermittent plug-flow pulses. Blue-dashed lines bound the electroactive region (EAR) over which the current collector extends. The equilibrium state-of-charge at the discharge cutoff voltage (0.5 V) is indicated by maroon-dashed lines.

Table S1 Projected energy density projection for various energy storage systems based on reactants only.

System	Average Voltage (V)	Energy Density (Wh/kg)	Energy Density (Wh/L)
Vanadium Redox Flow Batteries	1.5	50	40
Aqueous Li-ion Chemistry			
$LiTi_2(PO_4)_3$/ $LiFePO_4$	0.9	63	202
$LiTi_2(PO_4)_3$/ $LiMn_2O_4$	1.5	90	313
Aqueous Na-ion Chemistry			
$NaTi_2(PO_4)_3$/ $Na_{0.44}MnO_2$	1	33	127

Table S2 The simulated and experimental capacities with respect to cycle number for plug flow with flow volume factor m=1. The simulated 1st cycle charge capacity for suspension A are normalized to 150 mAh/g, other simulated capacities are scaled by the same factor.

Cycle number	Charge Capacity (mAh/g, LFP)		Discharge Capacity (mAh/g, LFP)	
	Suspension A	Suspension B	Suspension A	Suspension B
Simulation				
1	150.0	143.3	142.5	135.3
2	144.6	140.0	143.1	137.0
3	144.5	139.5	143.4	137.6
Experiment				
1	133	130	122	91
2	123	117	120	98
3	112	116	121	83

References

1. M. Duduta, B. Ho, V. C. Wood, P. Limthongkul, V. E. Brunini, W. C. Carter, and Y. Chiang, *Adv. Energy Mater.*, 2011, **1**, 511–516.
2. V. E. Brunini, Y.-M. Chiang, and W. C. Carter, *Electrochimica Acta*, 2012, **69**, 301–307.
3. J. Newman and K. E. Thomas-Alyea, *Electrochemical Systems*, John Wiley & Sons, 2004.
4. U. S. Kasavajjula, C. Wang, and P. E. Arce, *J. Electrochem. Soc.*, 2008, **155**, A866–A874.

Electronic Supplementary Material (ESI) for Physical Chemistry Chemical Physics
This journal is © The Owner Societies 2013

5. A. Aatiq, M. Ménétrier, L. Croguennec, E. Suard, and C. Delmas, *J. Mater. Chem.*, 2002, **12**, 2971–2978.
6. S. Patankar, *Numerical Heat Transfer and Fluid Flow*, Taylor & Francis, 1st edn., 1980.